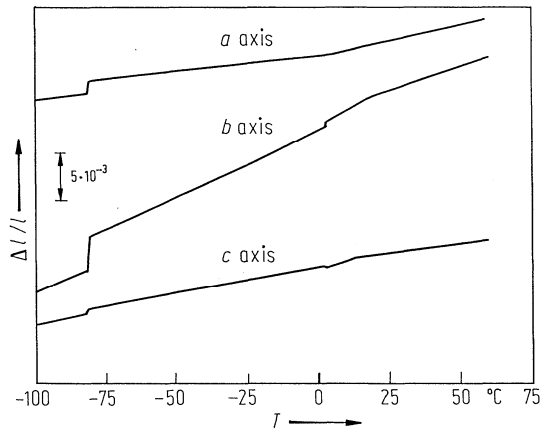

Fig. 39A-8-001. $[N(CH_3)_4]_2CoCl_4$. $\Delta l/l$ vs. T [85Saw]. $\Delta l/l$: linear thermal expansion along the a, b and c axes.

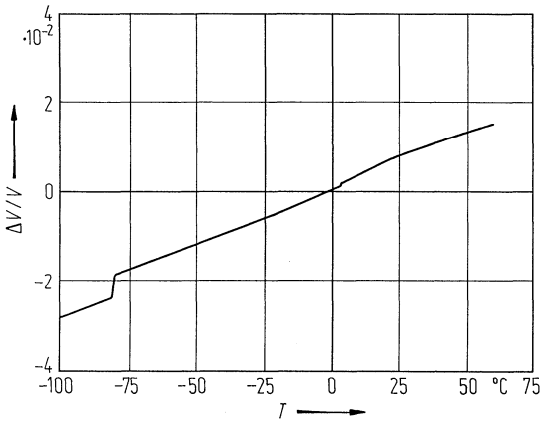

Fig. 39A-8-002. $[N(CH_3)_4]_2CoCl_4$. $\Delta V/V$ vs. T [85Saw]. $\Delta V/V$: volume thermal expansion.

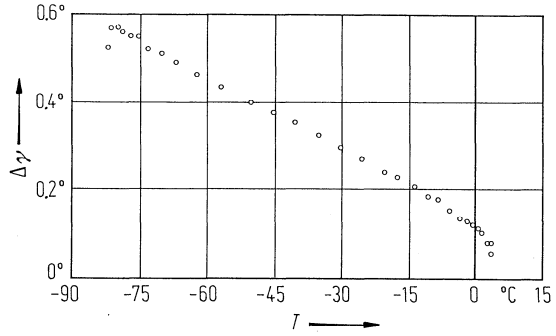

Fig. 39A-8-003. $[N(CH_3)_4]_2CoCl_4$. $\Delta\gamma$ vs. T [82Has]. $\Delta\gamma$: deviation of axial angle γ from 90°.

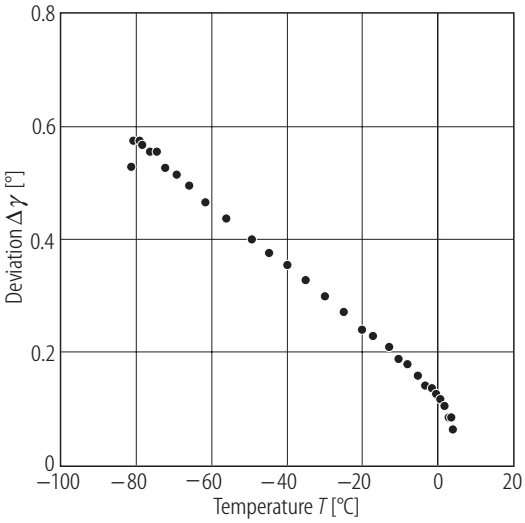

Fig. 39A-8-004. $[N(CD_3)_4]_2CoCl_4$. $\Delta\gamma$ vs. T [84Has]. $\Delta\gamma$: deviation of axial angle γ from 90°.

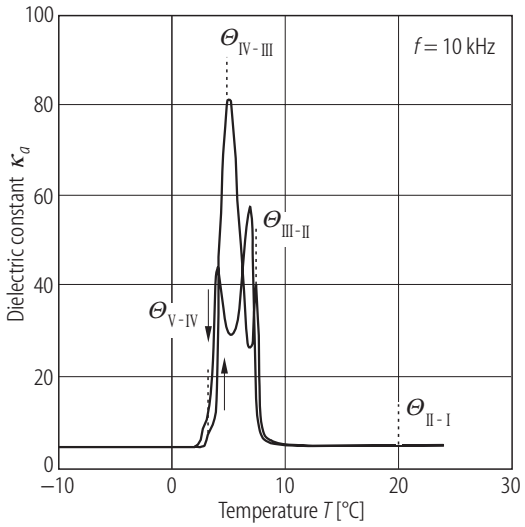

Fig. 39A-8-005. $[N(CH_3)_4]_2CoCl_4$. κ_a vs. T around phase III [85Saw].

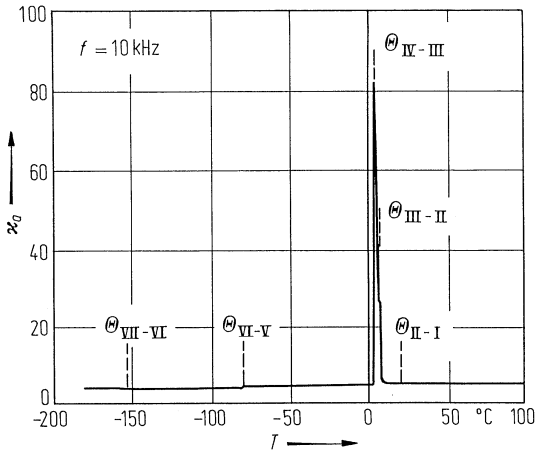

Fig. 39A-8-006. $[N(CH_3)_4]_2CoCl_4$. κ_a vs. T [85Saw]. On heating.

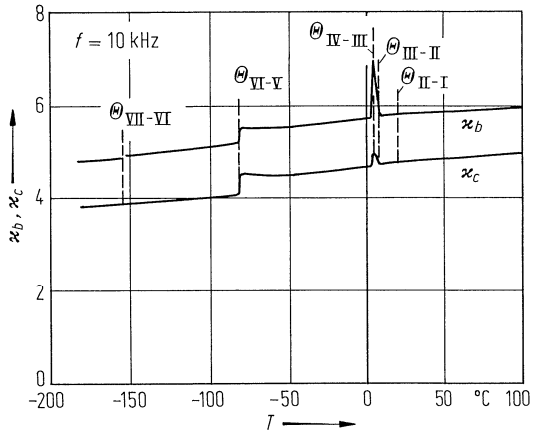

Fig. 39A-8-007. $[N(CH_3)_4]_2CoCl_4$. κ_b, κ_c vs. T [85Saw]. On heating.

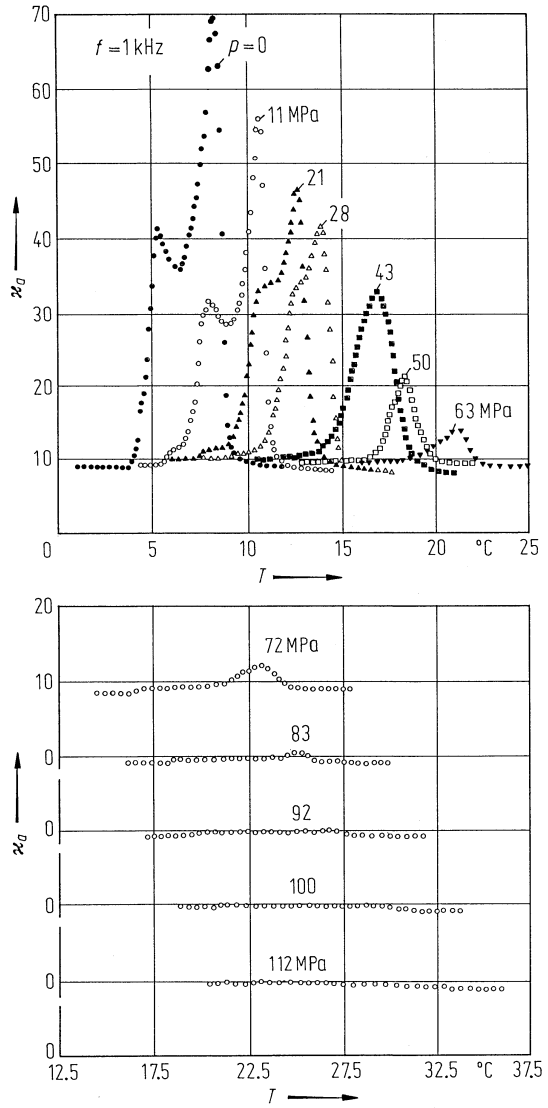

Fig. 39A-8-008. $[N(CH_3)_4]_2CoCl_4$. κ_a vs. T [80Shi]. Parameter: p. On cooling.

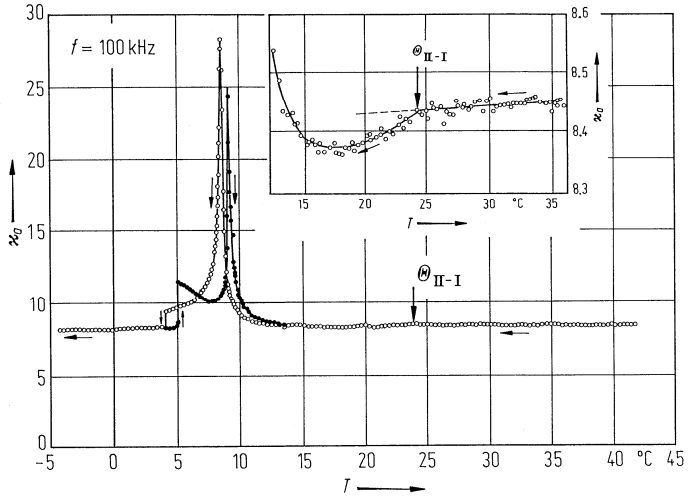

Fig. 39A-8-009. $[N(CD_3)_4]_2CoCl_4$. κ_a vs. T [82Ges2].

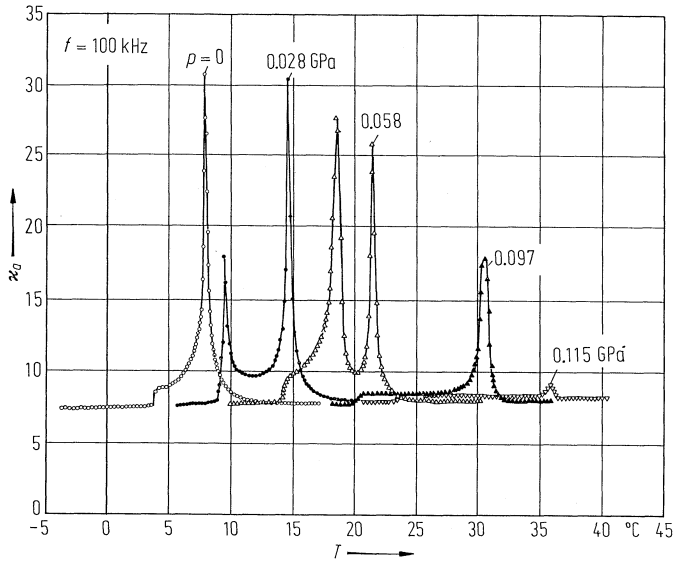

Fig. 39A-8-010. $[N(CD_3)_4]_2CoCl_4$. κ_a vs. T [82Ges1]. Parameter: p.

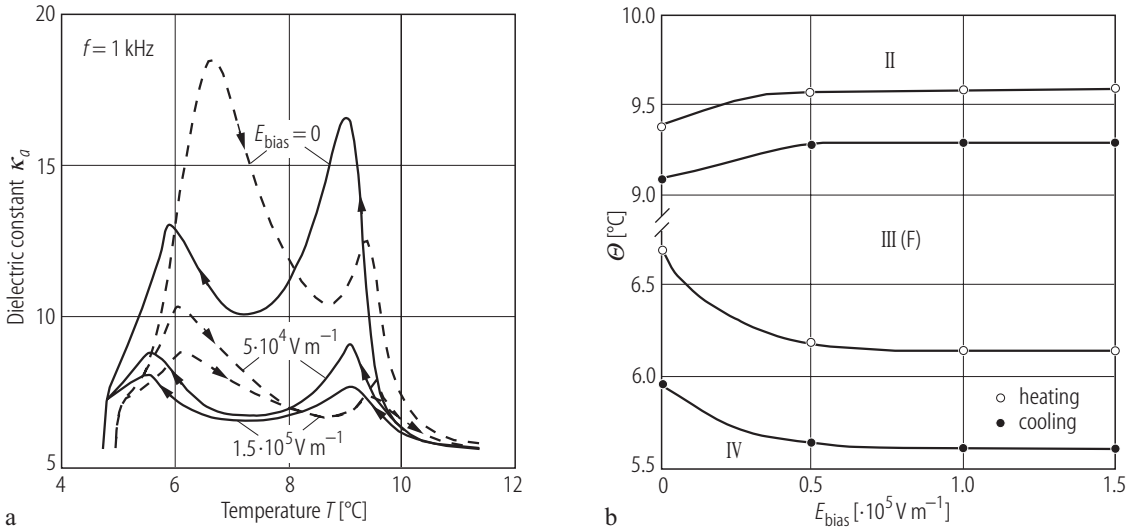

Fig. 39A-8-011. $[N(CH_3)_4]_2CoCl_4$. (**a**) κ_a vs. T [90Kal]. Parameter: E_{bias}. (**b**) Θ vs. E_{bias}.

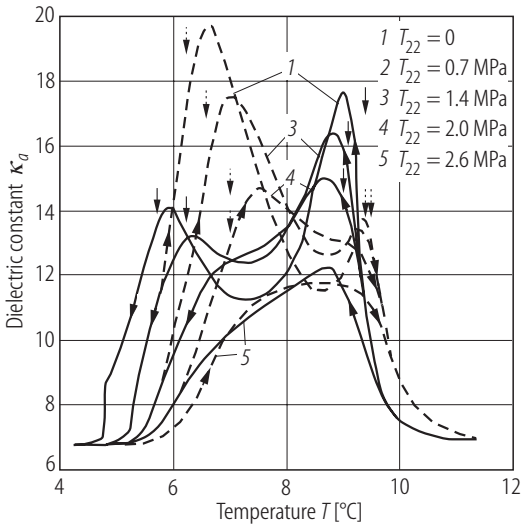

Fig. 39A-8-012. $[N(CH_3)_4]_2CoCl_4$. κ_a vs. T [91Gla]. Parameter: T_{22}. T_{22}: uniaxial stress along the b axis. Vertical arrows show high- and low-temperature boundaries of the ferroelectric phase.

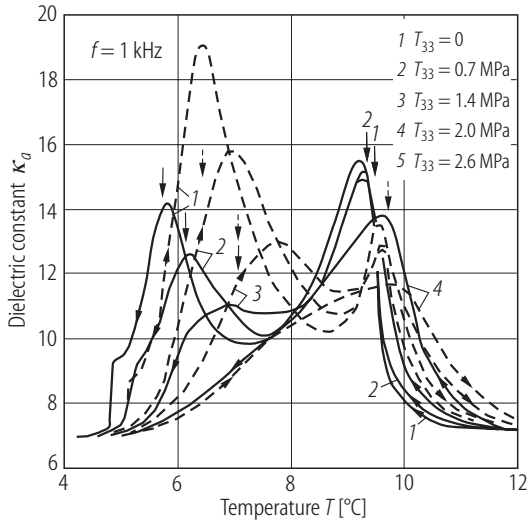

Fig. 39A-8-013. $[N(CH_3)_4]_2CoCl_4$. κ_a vs. T [91Gla]. Parameter: T_{33}. T_{33}: uniaxial stress along the c axis. Vertical arrows show high- and low-temperature boundaries of the ferroelectric phase.

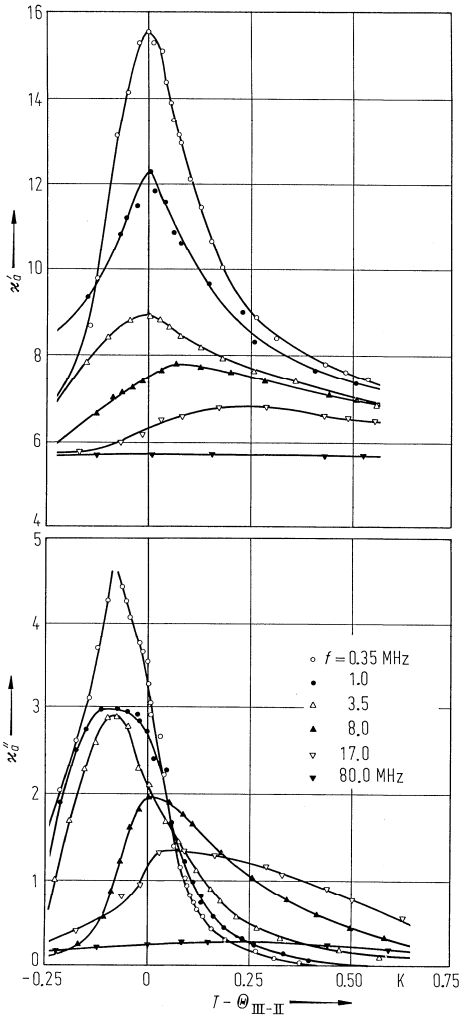

Fig. 39A-8-014. $[N(CH_3)_4]_2CoCl_4$. κ_a', κ_a'' vs. $T - \Theta_{III-II}$ [85Jak]. Parameter: f.

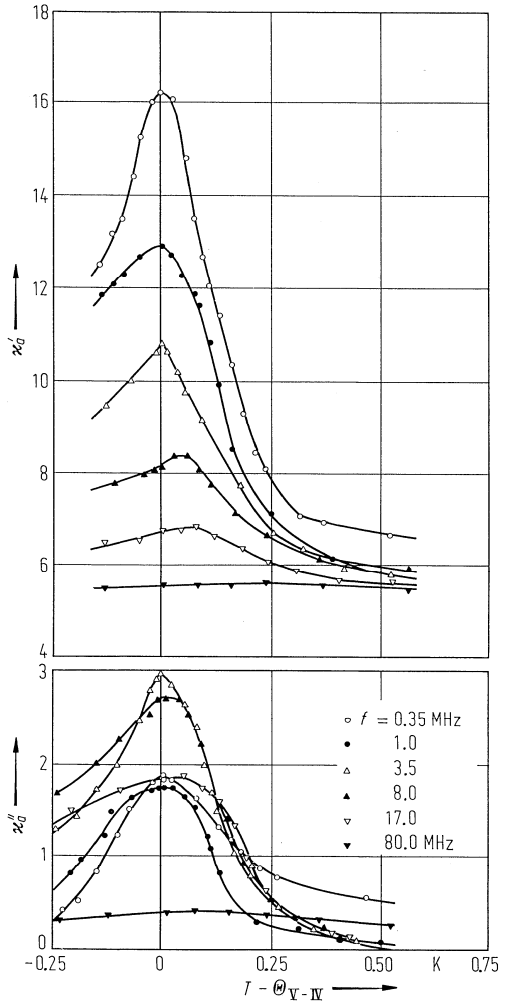

Fig. 39A-8-015. $[N(CH_3)_4]_2CoCl_4$. κ_a', κ_a'' vs. $T - \Theta_{V-IV}$ [85Jak]. Parameter: f.

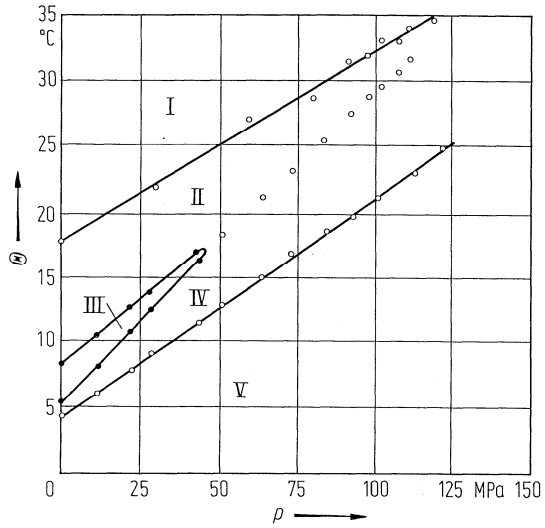

Fig. 39A-8-016. $[N(CH_3)_4]_2CoCl_4$. Θ vs. p [80Shi].

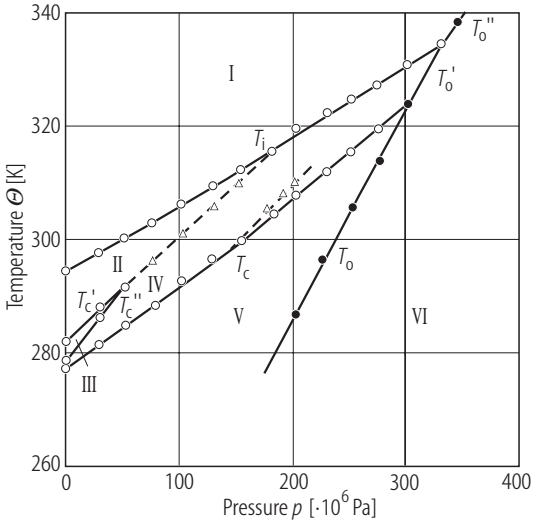

Fig. 39A-8-017. $[N(CH_3)_4]_2CoCl_4$. Θ vs. p [90Vlo].

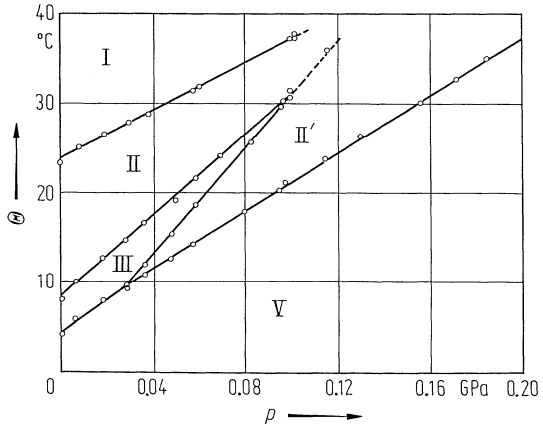

Fig. 39A-8-018. $[N(CD_3)_4]_2CoCl_4$. Θ vs. p [82Ges1].

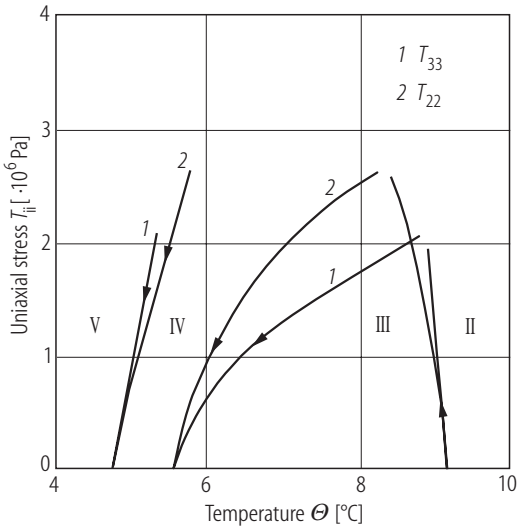

Fig. 39A-8-019. $[N(CH_3)_4]_2CoCl_4$. T_{ii} vs. Θ [92Gla]. T_{ii}: uniaxial stress.

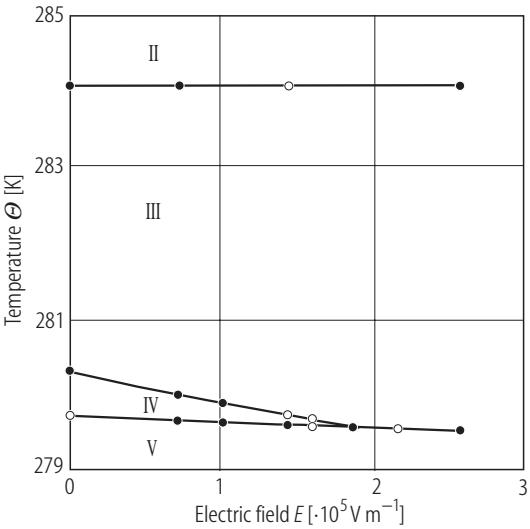

Fig. 39A-8-020. $[N(CH_3)_4]_2CoCl_4$. Θ vs. E in the vicinity of phase III and phase IV [93Sve].

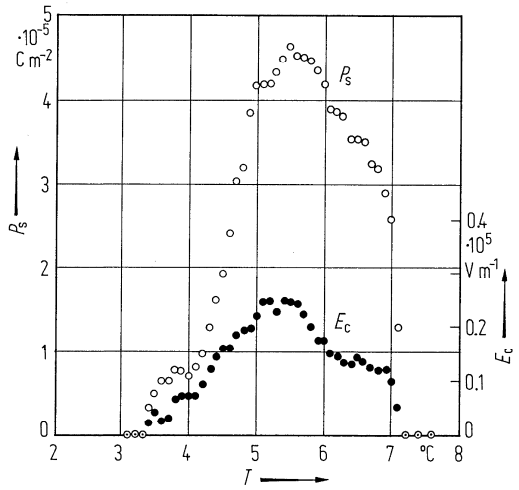

Fig. 39A-8-021. $[N(CH_3)_4]_2CoCl_4$. P_s, E_c vs. T [78Saw].

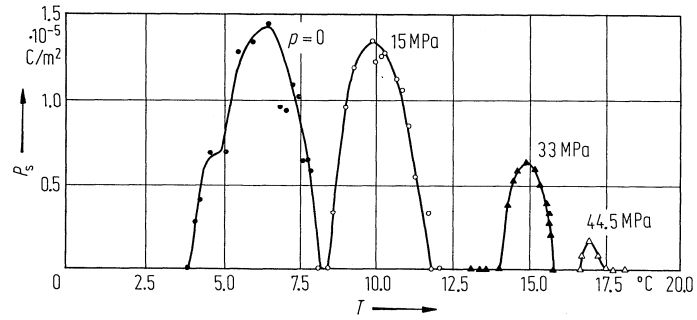

Fig. 39A-8-022. $[N(CH_3)_4]_2CoCl_4$. P_s vs. T [79Shi]. Parameter: p.

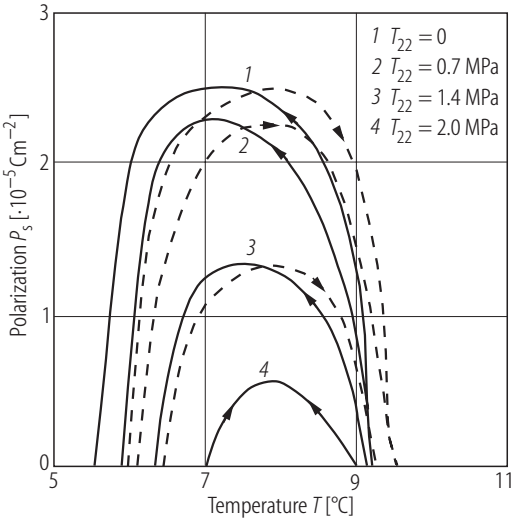

Fig. 39A-8-023. $[N(CH_3)_4]_2CoCl_4$. P_s vs. T [91Gla]. Parameter: T_{22}. T_{22}: uniaxial stress along the *b* axis.

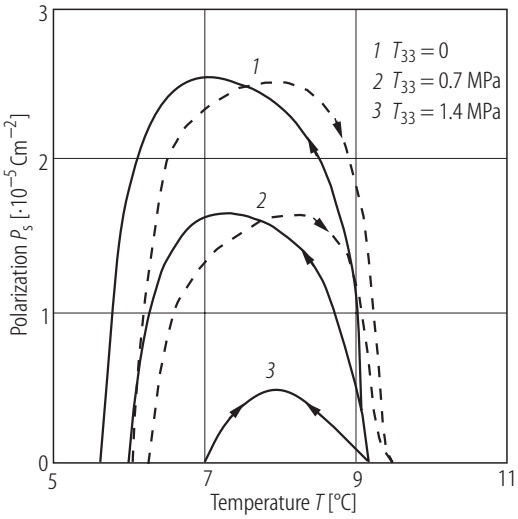

Fig. 39A-8-024. $[N(CH_3)_4]_2CoCl_4$. P_s vs. T [91Gla]. Parameter: T_{33}. T_{33}: uniaxial stress along the *c* axis.

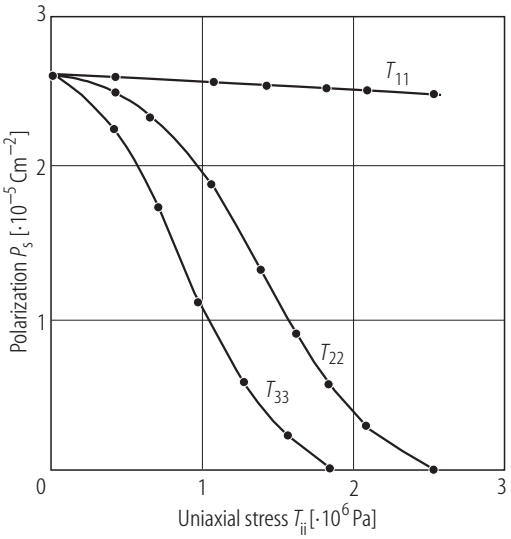

Fig. 39A-8-025. $[N(CH_3)_4]_2CoCl_4$. P_s vs. T_{ii} [91Gla]. T_{ii}: uniaxial stress.

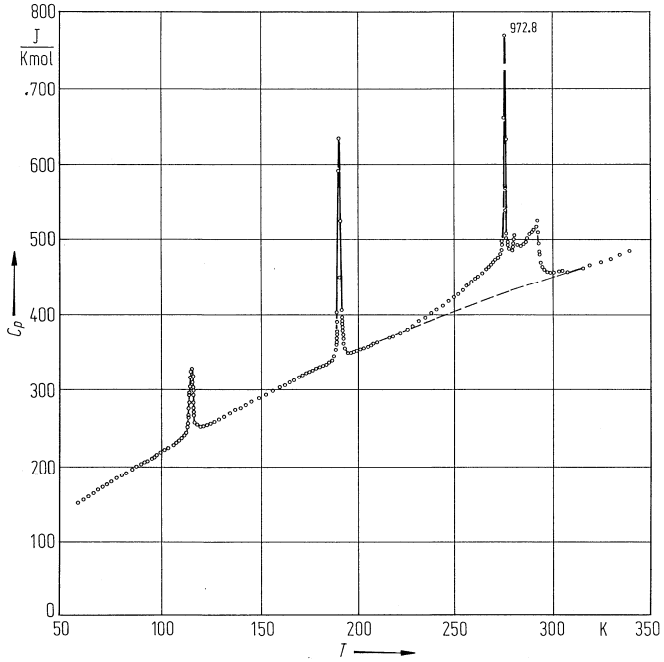

Fig. 39A-8-026. $[N(CH_3)_4]_2CoCl_4$. C_p vs. T [81Gom]. C_p: molar heat capacity at constant pressure.

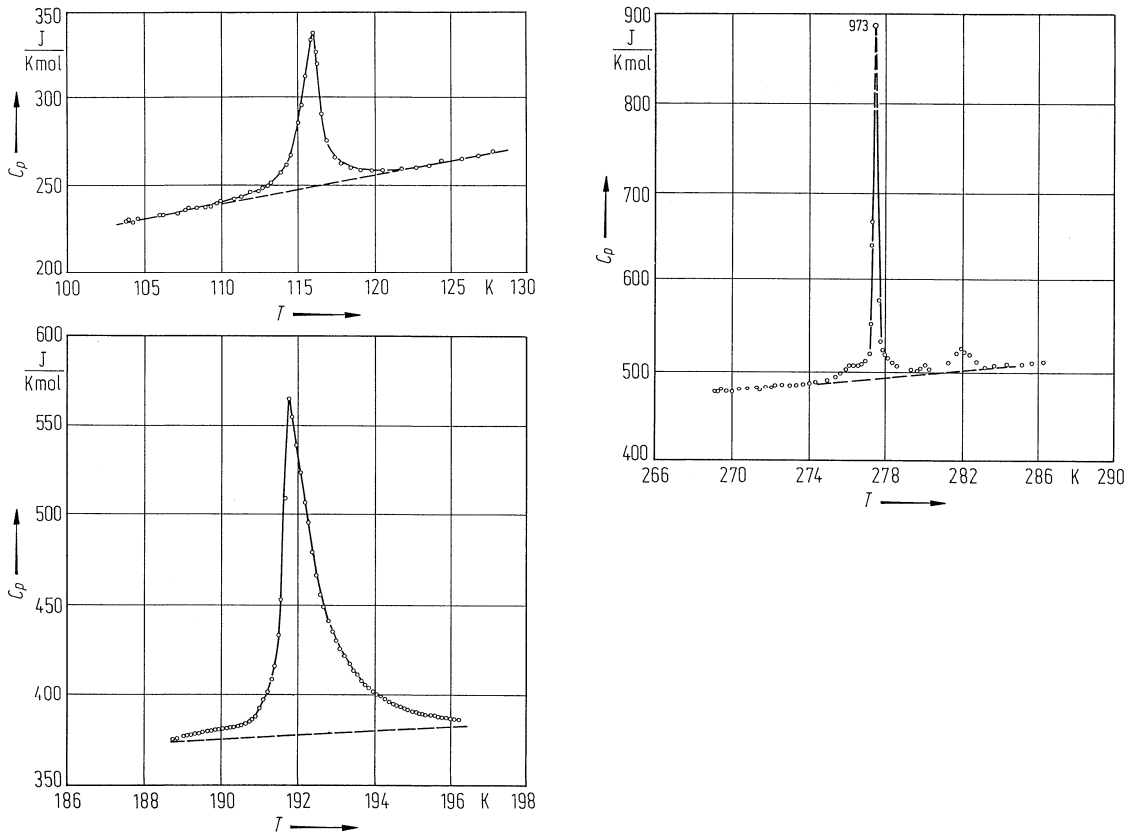

Fig. 39A-8-027. $[N(CH_3)_4]_2CoCl_4$. C_p vs. T around transition temperatures [81Gom]. C_p: molar heat capacity at constant pressure.

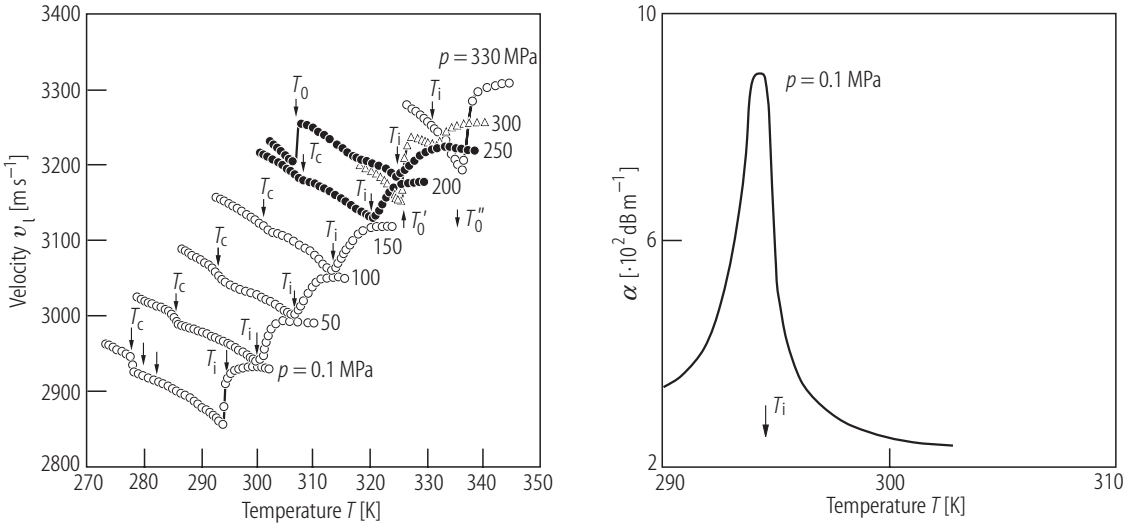

Fig. 39A-8-028. $[N(CH_3)_4]_2CoCl_4$. v_1, α vs. T [90Vlo]. v_1: velocity of longitudinal sound propagating in the [001] direction. α: attenuation coefficient of the sound velocity. Parameter: p. For T_c, T_i, T_0, T_0', T_0'' see Fig. 39A-8-017.

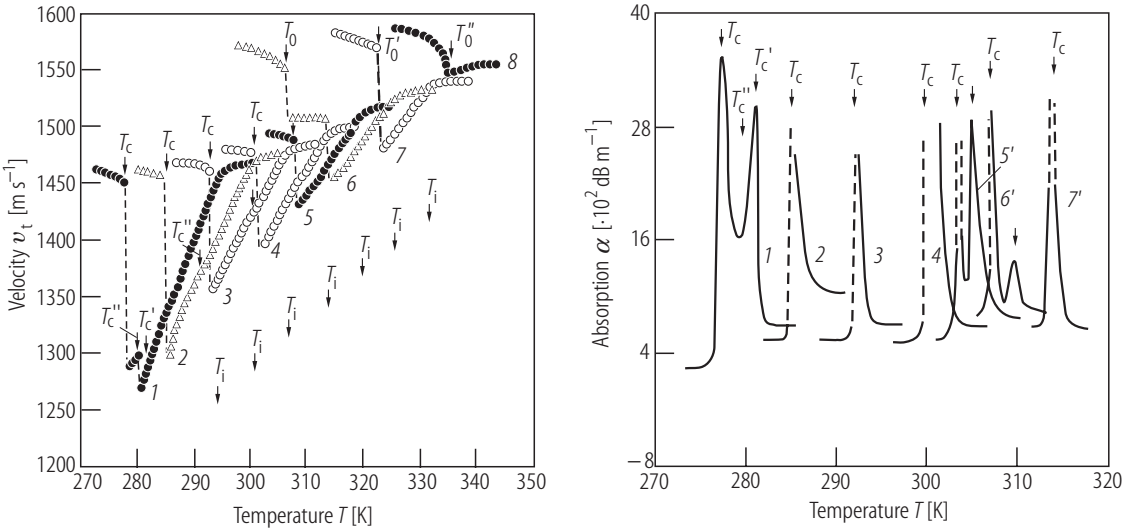

Fig. 39A-8-029. $[N(CH_3)_4]_2CoCl_4$. v_t, α vs. T [90Vlo]. v_t: velocity of the c_{44}-mode sound. α: attenuation coefficient. f = 10 MHz. *1*: 0.1 MPa, *2*: 50 MPa, *3*: 100 MPa, *4*: 150 MPa, *5*: 200 MPa, *6*: 250 MPa, *7*: 300 MPa, *8*: 330 MPa, *5′*: 175 MPa, *6′*: 190 MPa, *7′*: 250 MPa. For T_c, T_i, T_0, T_0', T_0'' see Fig. 39A-8-017.

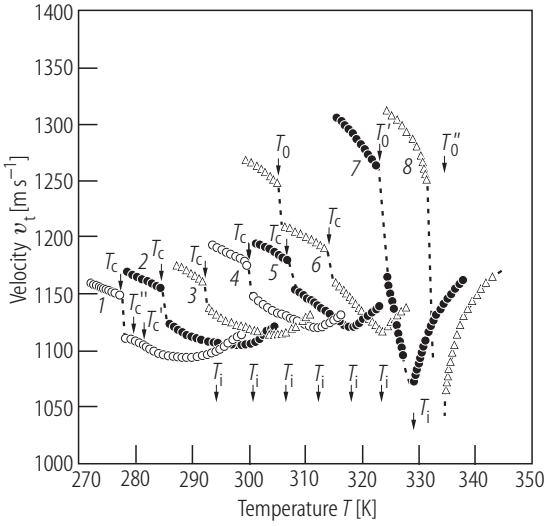

Fig. 39A-8-030. $[N(CH_3)_4]_2CoCl_4$. v_t vs. T [90Vlo]. v_t: velocity of the c_{55}-mode sound. f = 10 MHz. *1*: 0.1 MPa, *2*: 50 MPa, *3*: 100 MPa, *4*: 150 MPa, *5*: 200 MPa, *6*: 250 MPa, *7*: 300 MPa, *8*: 330 MPa. For T_c, T_i, T_0, T_0', T_0'' see Fig. 39A-8-017.

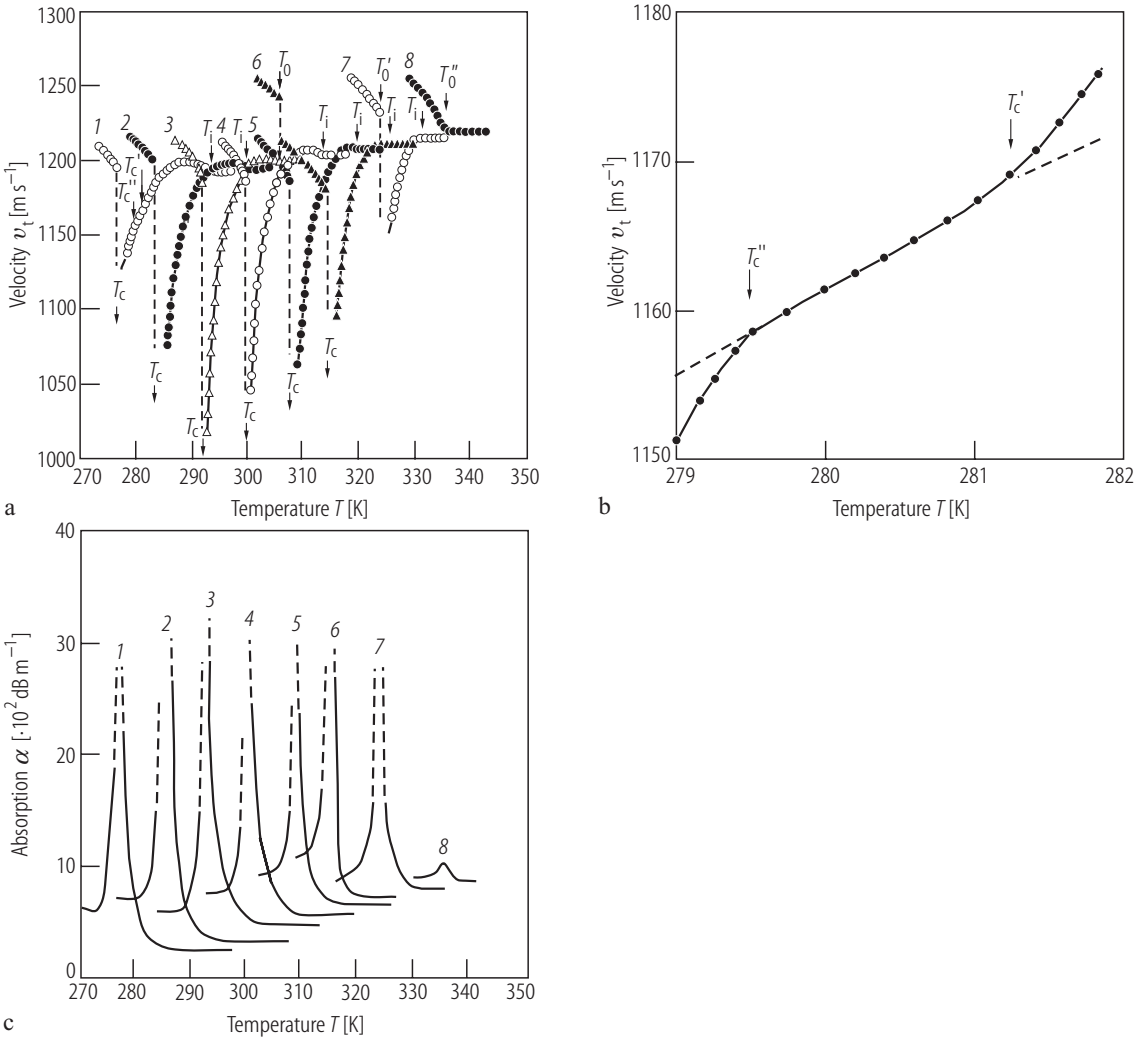

Fig. 39A-8-031. $[N(CH_3)_4]_2CoCl_4$. (**a**), (**b**) v_t vs. T, (**c**) α vs. T [90Vlo]. v_t: velocity of the c_{66}-mode sound. α: attenuation coefficient. f = 10 MHz. *1*: 0.1 MPa, *2*: 50 MPa, *3*: 100 MPa, *4*: 150 MPa, *5*: 200 MPa, *6*: 250 MPa, *7*: 300 MPa, *8*: 330 MPa. (**b**) Expanded view for 0.1 MPa. For T_c, T_i, T_0, T_0', T_0'' see Fig. 39A-8-017.

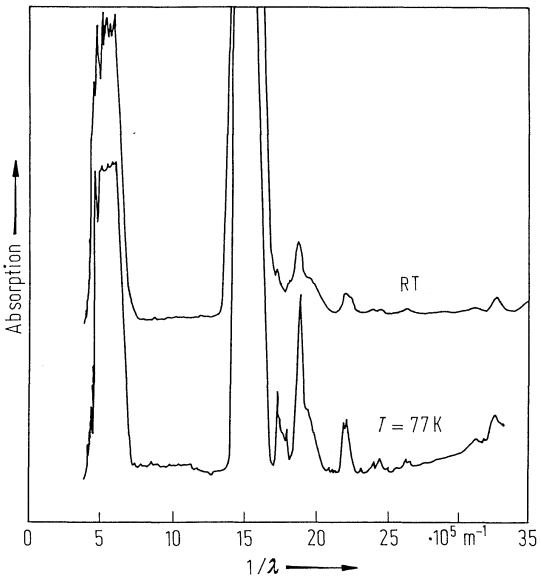

Fig. 39A-8-032. $[N(CH_3)_4]_2CoCl_4$. Absorption vs. $1/\lambda$ [86Koj].

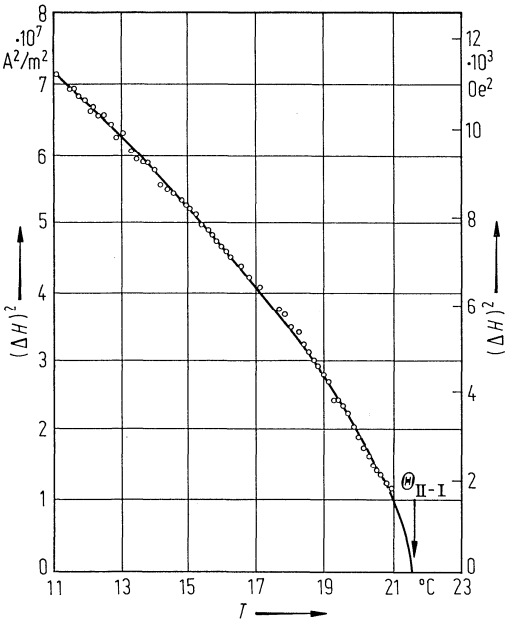

Fig. 39A-8-033. $[N(CH_3)_4]_2CoCl_4$. $(\Delta H)^2$ vs. T [82Tsu]. ΔH: edge separation of the ESR line of Mn^{2+}.

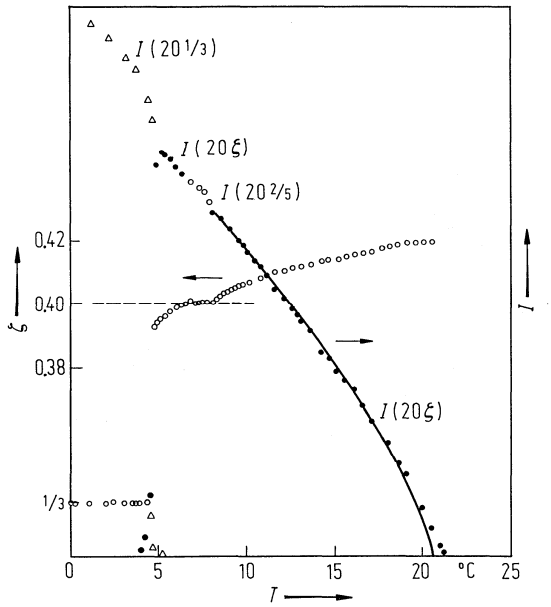

Fig. 39A-8-034. $[N(CH_3)_4]_2CoCl_4$. I, ζ vs. T [80Has]. I: integrated intensities of X-ray reflections at (2, 0, ζ); ζ: modulation wavenumber in unit of c^*.

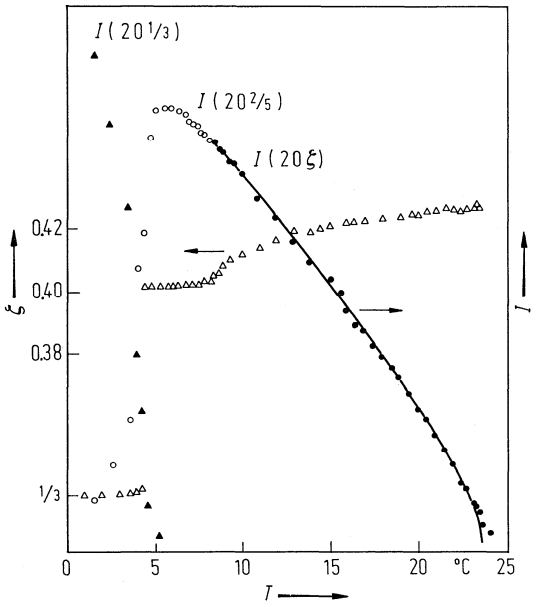

Fig. 39A-8-035. $[N(CD_3)_4]_2CoCl_4$. I, ζ vs. T [84Has]. I: integrated intensities of X-ray reflections at (2, 0, ζ); ζ: modulation wavenumber in unit of c^*.